Jaatinen, Salla; Touronen, Jouni; Karinen, Reetta; Uusi-Kyyny, Petri; Alopaeus, Ville

Hydrogen solubility in furfural and 2-propanol

Please cite the original version:
Jaatinen, S., Touronen, J., Karinen, R., Uusi-Kyyny, P., & Alopaeus, V. (2017). Hydrogen solubility in furfural and 2-propanol: Experiments and modeling. *Journal of Chemical Thermodynamics*, *112*, 1-6. https://doi.org/10.1016/j.jct.2017.04.004

HYDROGEN SOLUBILITY IN FURFURAL AND 2-PROPANOL: EXPERIMENTS AND MODELING

Salla Jaatinen, Jouni Touronen, Reetta Karinen, Petri Uusi-Kyyny, Ville Alopaeus

Aalto University, School of Chemical Engineering, Department of Chemical and Metallurgical Engineering, P.O. Box 16100, FI-00076 Aalto, FINLAND
* salla.jaatinen@aalto.fi

ABSTRACT

Production of valuable chemicals from furfural through hydrotreatment requires information of hydrogen solubility in furfural and the most often applied solvent, 2-propanol. This study investigates hydrogen solubility in furfural and 2-propanol at the temperature range of 323 - 476 K and pressure range up to 12.5 MPa. The measured data are compared to prediction with Soave-Redlich-Kwong, Peng-Robinson, and Perturbed-Chain Statistically Associating Fluid Theory (PC-SAFT) equations of state. The most accurate prediction of hydrogen solubility in furfural and 2-propanol was obtained with PC-SAFT.

Keywords: Furfural, hydrogen, 2-propanol, solubility, GLE, PC-SAFT

Nomenclature

A	Parameter for density or vapor pressure in DIPPR correlation
AAD	Average absolute deviation (MPa)
B	Parameter for density or vapor pressure in DIPPR correlation
C	Parameter for density or vapor pressure in DIPPR correlation
D	Parameter for density or vapor pressure in DIPPR correlation
E	Parameter for vapor pressure in DIPPR correlation
FID	Flame ionization detector
GC	Gas chromatography
k_{ij}	Binary interaction parameter
m	PC-SAFT segment diameter parameter
MS	Mass spectrometer
P	Pressure (MPa)
P_c	Critical pressure (MPa)
PC-SAFT	Perturbed-chain statistically associating fluid theory
PR	Peng-Robinson
RAD	Relative average deviation (%)
SRK	Soave-Redlich-Kwong
T	Temperature (K)
T_c	Critical temperature (K)
V_m	Ideal gas molar volume NTP (22 414 cm^3 mol^{-1})
x	Mole fraction
Greek letters	
ω	Acentric factor
ε/k	PC-SAFT segment energy parameter (K)
ρ_L	Liquid density (mol cm^{-1})
σ	PC-SAFT number of segments parameter (Å)

1. Introduction

The potential of lignocellulosic biomass conversion for the production of valuable chemicals and fuels has been acknowledged for decades. Lignocellulosic biomass offers a sustainable platform for chemical production from renewable feedstocks, one of those being furfural. Furfural has been recognized as a potential building block for production of multiple value-added chemicals and fuels. This chemical can be produced from hemicellulose, a part of lignocellulosic biomass.[1-4] A variety of reaction routes exist to convert furfural to many valuable products. One potential reaction route is hydrotreatment of furfural. Potential products through furfural hydrotreatment include furfuryl alcohol, tetrahydrofurfuryl alcohol, and 2-methylfuran. These components have applications as solvents, resin materials, and specialty chemicals in medical industry, and even as biofuels.[4,5]

Furfural hydrotreatment has a complex reaction scheme, and reaction conditions as well as catalysts applied in the reaction must be optimized to achieve the desired reaction route. Furfural hydrotreatment can be performed in gas or liquid phase, both having favorable properties. High yields of products have been achieved in gas phase reactions, but liquid phase reaction offers easier merging to upstream production of furfural.[6,7] The knowledge of reaction mechanisms and kinetics give valuable information about the desired reactions. The knowledge of kinetics is especially important to enable the scale up of processes. For the kinetics, one of the important parameters is the hydrogen solubility in the reaction medium and furfural. Especially in the liquid phase processes, the amount of hydrogen dissolved can be a factor restricting the reactions from occurring. In addition, furfural hydrogenation experiments in the liquid phase can suffer from material balance uncertainties, which accurate phase equilibria models can substantially improve.[5,8,9]

Furfural hydrotreatment reactions are usually studied in a solvent and one of the most applied solvents in the hydrotreatment studies is 2-propanol.[10,11] Hydrogen solubility in 2-propanol has been studied earlier for example by Lühring et al.[12] at 293.2 K and Krüger et al.[13] at 298.15 K. Hydrogen solubility in furfural has remained unstudied in the past.

To attain important information for pure furfural and 2-propanol, the measured hydrogen solubility data should be described with a model. With alcohols, including 2-propanol, many different predictive and equations of state models have been applied in earlier studies e.g. Soave-Redlich-Kwong (SRK)[14] and Peng-Robinson (PR).[15-18] The same models applied for 2-propanol might not be suitable for furfural due to molecular differences and characteristics. Thus, in this study the obtained hydrogen solubility data are tested with three equation of state models: SRK, PR, and Perturbed-Chain Statistical Associating Fluid Theory (PC-SAFT)[19]. SRK and PR are cubic equations of state and mostly recommended for gas-

processing, refinery, and petrochemical applications.[14,15] SRK and PR in their traditional forms are suitable for nonpolar or mildly polar mixtures, thus the suitability for intermediately polar furfural is unclear. PC-SAFT is an equation of state model that uses second-order perturbation theory of Barker and Henderson [20,21] together with statistical associating fluid theory by Chapman et al. [22]. PC-SAFT is applicable for fluid systems of small and/or large molecules and the temperature and pressure range for this model is wide.[19,23] Oxygenated compounds or polar systems might cause problems to some predictive models, but PC-SAFT has been reported to function well in these cases.[24-26] PC-SAFT has been employed to model phase equilibrium and hydrogen solubility in a variety of liquids with excellent predictive capability.[19,23-29]

This study reports new hydrogen solubility data in furfural and 2-propanol at temperatures of 323, 399, and 476 K in the pressure range of 0.3 – 12.5 MPa. Furthermore, a comparison of SRK, PR, and PC-SAFT models for predicting the hydrogen solubility in furfural and 2-propanol is conducted. This new data will provide important information for modeling furfural hydrotreatment reactions.

2. Experimental

2.1. Materials

The components and their purities are presented in Table 1. Due to the low stability of furfural, it was purified with vacuum distillation procedure at 55 mbar and bottom boiler temperature of 355 K. Furfural was distilled into three fractions: light, middle, and the heavy distillate fractions. Light and heavy distillates were discarded and middle distillate was used in the phase equilibrium study. The amount of light distillate discarded was approximately 100 cm^3. The color of furfural before the distillation was light brown due to known resinification and oxidation reactions, but after the distillation the chemical was nearly colorless with some hint of yellow color. The purity of distilled furfural was analyzed with gas chromatography. 2-propanol and hydrogen were used without any purification.

Table 1

Chemical, CAS number, supplier, initial and final purity, and analysis method for purity.

Chemical	CAS number	Supplier	Initial mole fraction purity[a]	Purification method	Final mole fraction purity[b]	Analysis method
Furfural	98-01-1	Sigma-Aldrich	0.99	Distillation	0.998	GC
2-Propanol	67-63-0	Sigma-Aldrich	≥ 0.995	None	-	-

| Hydrogen | 1333-74-0 | AGA | 0.99999 | None | - | - |

2.2. Apparatus

A continuous flow apparatus was applied to measure the solubility of hydrogen in furfural and 2-propanol. This apparatus has been described in detail by Saajanlehto et al. [30]. The temperature in the experiments was measured with a type K thermocouple and the standard uncertainty of the temperature measurements was ± 0.2 K according to a calibration. The thermocouple calibration was performed with a Pt-100 temperature probe and a Tempcontrol F200 thermometer. The pressure was measured with a pressure transducer (Trafag NAH 8253) and the standard uncertainty of the pressure measurements was ± 0.02 MPa according to a calibration. Calibration was performed with Beamex MC2-PE calibrator equipped with an external pressure module (EXT60). Both the thermometer and the pressure calibrator were calibrated by the Finnish National Standards Laboratory (MIKES).

2.3. Measurement procedure

The hydrogen solubility data in pure furfural and 2-propanol were collected by employing the continuous flow apparatus. The measurements were made at the temperatures of 323, 399, and 476 K in the pressure range of 0.3 – 12.5 MPa. The highest temperature (476 K) is a usual furfural hydrogenation temperature and thus chosen for the analysis. The lowest temperature (323 K) is in a range, where the furfural reactions are assumed basically non-existent. The middle temperature (399 K) was chosen between the temperature range to obtain information of the temperature behavior and amount of hydrogenated products as a function of temperature. Before the experiments, furfural or 2-propanol was weighed and degassing was performed for the component under vacuum in an ice bath for one hour to remove dissolved gases from the sample. Hydrogen + liquid with predetermined molar fraction of hydrogen was prepared within the continuous flow apparatus by injecting hydrogen gas into the liquid stream of furfural or 2-propanol. The limit of hydrogen solubility was determined by varying the gas flow of hydrogen and identifying the amount of phases (gas-liquid or liquid) within the view cell of the apparatus by visual observation. Figure 1a presents the two-phase region with hydrogen bubble in a hydrogen solubility experiment with the continuous flow apparatus. Figure 1b presents the liquid phase.
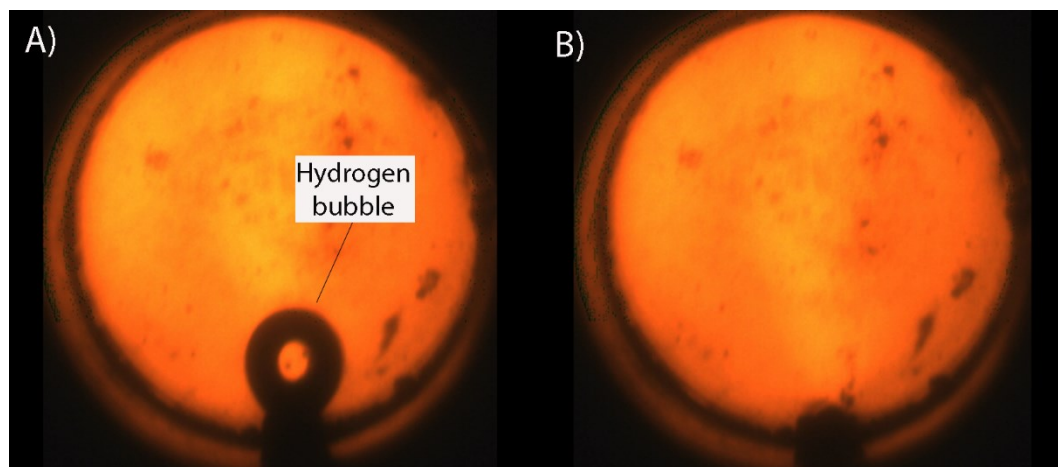
Figure 1. a) Two-phase region with hydrogen bubble, b) liquid phase in hydrogen solubility experiment.

Thermal reactions of furfural were suppressed with the short residence time of the hydrogen + liquid mixture in the equilibrium cell. The residence time used in the measurements varied between 2.2 and 11.8 min depending on the liquid flow rate. Sufficiency of residence time and settling of phase equilibrium was confirmed by repeating some of the measurements with varying fluid and gas flow rates. To confirm that no thermal reactions of relatively unstable furfural had occurred during the measurement, liquid samples were taken before and after the measurement and the samples were analyzed with gas chromatography. The quantitative analysis was performed with a gas chromatograph equipped with a flame ionization detector (GC-FID, Agilent 6890) and a Zebron ZB-wax Plus column (60 m x 0.25 mm x 0.25 µm). The temperature ramp with GC was from 313.15 K to 373.15 K with the heating rate of 5 K min^{-1} and from 313.15 K to 513.15 K with the heating rate of 20 K min^{-1}. Injection volume and temperature were 1 µl and 503.15 K, respectively. 2-butanol was used as an internal standard. The qualitative analysis of liquid phase components was performed with a GC-MS (Agilent 7890-5975) by applying a similar column and method. The mass spectra was recorded in electron impact ionization at 70 eV.

2.4. Density and vapor pressure calculations

For calculating the density and vapor pressure of pure liquid components, DIPPR correlations were applied. [31] The correlation equations and the parameters are presented in the supplementary information (Equations S1 and S2, Table S1). The calculated uncertainty for furfural density from DIPPR datasets at low temperatures is less than 0.4 % and for 2-propanol less than 0.07 %. The values were calculated as standard uncertainties from reported values. The calculated standard uncertainty for pure component vapor pressure from DIPPR datasets for furfural is 3 % and for 2-propanol < 1.5 %. The calculated vapor pressures are presented later together with the hydrogen solubility data.

2.5. Hydrogen solubility

Mole fraction of hydrogen in the total flow was calculated with Equation 1 applying liquid and gas flow rates.

$$x_{H2} = \frac{\dfrac{H_{2,FLOW}}{V_m}}{L_{FLOW}\,\rho_L + \dfrac{H_{2,FLOW}}{V_m}} \tag{1}$$

where x_{H2} is the mole fraction of hydrogen in the total flow, $H_{2,FLOW}$ is the hydrogen flow measured with a mass flow controller (cm^3 min^{-1}), V_m is the ideal gas molar volume (22 414 cm^3 mol^{-1}), L_{FLOW} is the volumetric liquid flow (cm^3 min^{-1}), and ρ_L is the liquid density (mol cm^{-3}).

The average of hydrogen mole fraction of the first observed point in the gas-liquid region and last observed point in the liquid phase region was calculated to determine the hydrogen solubility into furfural or 2-propanol (Equation 2). The uncertainty components taken into account in the uncertainty estimate in Equation 3 are presented in Table 2.

$$x_{H2} = \frac{x_{H2,L} + x_{H2,GL}}{2} \tag{2}$$

where x_{H2} is the solubility of hydrogen, $x_{H2,L}$ is the hydrogen mole fraction in the last point in the liquid region and $x_{H2,GL}$ is the hydrogen mole fraction in the first observed point in the gas-liquid region.

$$u(x_{H2}) = \left| \frac{\dfrac{L_{FLOW}\,\rho_L}{V_m}}{\left(\dfrac{H_{2,FLOW}}{V_m} + L_{FLOW}\,\rho_L\right)^2} \right| \Delta H_{2,FLOW} + \left| \frac{-\dfrac{H_{2,FLOW}\,\rho_L}{V_m}}{\left(\dfrac{H_{2,FLOW}}{V_m} + L_{FLOW}\,\rho_L\right)^2} \right| \Delta L_{FLOW} + \left| \frac{-\dfrac{H_{2,FLOW}\,L_{FLOW}}{V_m}}{\left(\dfrac{H_{2,FLOW}}{V_m} + L_{FLOW}\,\rho_L\right)^2} \right| \Delta \rho_L + \left| \frac{x_{H2,L} + x_{H2,GL}}{2} \right| \tag{3}$$

where $u(x_{H2})$ is the uncertainty of the hydrogen mole fraction, $\Delta H_{2,FLOW}$ is the uncertainty of the hydrogen flow rate, ΔL_{FLOW} is the uncertainty of the liquid flow rate, $\Delta \rho_L$ is the uncertainty of the liquid density. The last term on the right in Equation 3 is resulting from the method determining the bubble point composition by taking the difference of composition from the last point in the liquid region and the first observed point in the gas-liquid region.

Table 2

Uncertainty components applied in uncertainty calculations.

Uncertainty component	Value	Comments
$\Delta H_{2,FLOW}$	0.2 cm^3 min^{-1}	According to manufacturer.
ΔL_{FLOW}	0.5 % of the set-point	According to manufacturer.
$\Delta \rho_L$	0.4 % for furfural 0.07 % for 2-propanol	Comparison using measured density and the correlation [31], the largest deviation value from the accepted data was used.
$\left\| \dfrac{x_{H2,L} - x_{H2,GL}}{2} \right\|$	Observation dependent	The uncertainty caused by the composition distance of the last composition observed in the liquid phase region and the gas-liquid region.

3. Results and discussion

To investigate the hydrogen solubility in furfural and 2-propanol, data were collected at 323, 399, and 476 K in the pressure range of 0.3 – 12.5 MPa. Table 3 presents the experimental data points of hydrogen solubility in 2-propanol and Table 4 presents the hydrogen solubility in furfural.

Table 3

Measured hydrogen solubility in 2-propanol (x_{H2}) data points at temperature (T), pressure (P), and uncertainty of mole fraction of hydrogen in liquid ($u(x_{H2})$).

T / K	P / MPa	x_{H2}	$u(x_{H2})$
323.4	12.47	0.0347	0.0014
323.4 *	12.45	0.0350	0.0013
323.4	9.96	0.0288	0.0012
323.5	6.97	0.0199	0.0010
323.4	5.30	0.0139	0.0009
323.5 *	5.30	0.0139	0.0010
399.1	12.47	0.0501	0.0022
399.1	9.96	0.0395	0.0022
399.1	6.97	0.0305	0.0014
475.9	12.44	0.0637	0.0021
476.1	6.97	0.0365	0.0020

Standard uncertainties: u(T) = 0.2 K, u(P) = 0.02 MPa.
*Repeated measurements with changed fluid and gas flow rates.

Table 4

Measured hydrogen solubility in furfural (x_{H2}) data points at temperature (T), pressure (P), uncertainty of mole fraction of hydrogen in liquid ($u(x_{H2})$), and furfural purity analyzed with GC from the stabilization pump.

T / K	P / MPa	x_{H2}	$u(x_{H2})$	FUR purity / mole fraction
323.1	12.45	0.0138	0.0009	-
399.2	12.44	0.0290	0.0012	0.987
399.2	9.95	0.0229	0.0011	0.987
399.2	6.97	0.0154	0.0010	0.987
476.1	12.45	0.0381	0.0014	0.954
476.1	9.95	0.0305	0.0013	0.954
476.1	6.96	0.0229	0.0011	0.954

Standard uncertainties: u(T) = 0.2 K, u(P) = 0.02 MPa.

The repeatability of the experimental data points was evaluated by the repetitive measurements of two of the data points by varying the fluid and gas flow rates. The repeatability was surprisingly good as can be seen from Table 3. Also, the well known trend in hydrogen solubility was observed, as the solubility increased as a function of increasing pressure and temperature. This trend is observed in several previous studies.[17,32-35]

The experimental data were compared to the prediction with SRK, PR, and PC-SAFT models with Aspen Plus software.[36] Table 5 presents the pure component data applied for modeling. With PC-SAFT three parameters are required for all components; segment number (m), segment diameter (σ), and segment energy (ε/k). For furfural, pure component PC-SAFT parameters were regressed in Aspen applying vapor pressure and density data provided by NIST database.[31] Parameters for 2-propanol and hydrogen were obtained as such from Aspen software.[36]

The modeling was performed first by applying k_{ij} value of zero and then by applying a temperature independent binary interaction parameter value from the regression. The binary interaction parameter values (k_{ij}), average absolute deviation (AAD), and relative average deviation (RAD) with all the tested models are presented in Table 6. AAD and RAD equations applied for calculations are presented in Equations 4 and 5.

Table 5

Parameters of pure components for PR, SRK, and PC-SAFT models.[36]

Parameter	Furfural	2-Propanol	Hydrogen
P_c / MPa	5.66	4.77	33.19
T_c / K	670.150	508.300	1.313
Acentric factor ω	0.367784	0.663000	-0.215993
PC-SAFT segment number m_i	3.55759	3.07324	0.82850
PC-SAFT segment diameter σ_i / Å	3.18452	3.20028	2.97290
PC-SAFT segment energy ε_i/k / K	293.18452	209.54400	-260.62000

$$AAD = \frac{1}{N}\sum_{i=1}^{N}\left|P_{i,measured} - P_{i,calculated}\right| \tag{4}$$

$$RAD = \frac{100}{N}\sum_{i=1}^{N}\frac{\left|P_{i,measured} - P_{i,calculated}\right|}{P_{i,measured}} \tag{5}$$

Where N presents the number of observations and P_i presents the pressure (MPa).

Table 6

The temperature independent binary interaction parameters (k_{ij}), AAD and RAD values with SRK, PR, and PC-SAFT models.

Model	H₂ + Furfural			H₂ + 2-propanol		
	k_{ij}	AAD / MPa	RAD / %	k_{ij}	AAD / MPa	RAD / %
	0	1.18	11.5	0	1.26	12.2
SRK	0.291	0.91	8.5	-0.092	1.11	11.3
	0	1.90	18.8	0	1.48	15.3
Peng-Robinson	-0.371	1.17	11.0	-0.298	0.67	7.2
	0	3.12	30.3	0	2.82	30.4
PC-SAFT	-0.246	0.71	6.3	-0.277	0.54	5.3

In the comparison of SRK, PR, and PC-SAFT models in predicting hydrogen solubility in furfural and 2-propanol with binary interaction parameter zero, SRK model predicted the measured data the most accurately. However, the AAD and RAD values are relatively high, even SRK has RAD of 11.5 % for H₂

+ furfural and 12.2 % for H_2 + 2-propanol. On the other hand, as the binary interaction parameters were regressed, the PC-SAFT model predicted the measured data the most accurately with the lowest AAD and RAD values (Table 6). Further investigation of PC-SAFT data prediction indicated that the binary interaction parameters for H_2 + furfural and H_2 + 2-propanol are temperature dependent. Due to this, binary interaction parameters were regressed individually for each temperature. Table 7 presents the applied binary interaction parameters for PC-SAFT in each temperature. The measured hydrogen solubility data in 2-propanol, calculated vapor pressures of 2-propanol, as well as modeling with PC-SAFT with temperature dependent binary interaction parameters are presented in Figure 2. The experimental data points for hydrogen solubility in furfural, calculated vapor pressures of furfural, and the modeling with PC-SAFT are presented in Figure 3.

Table 7

Temperature dependent PC-SAFT binary interaction parameters for H_2 + furfural and H_2 + 2-propanol mixtures.

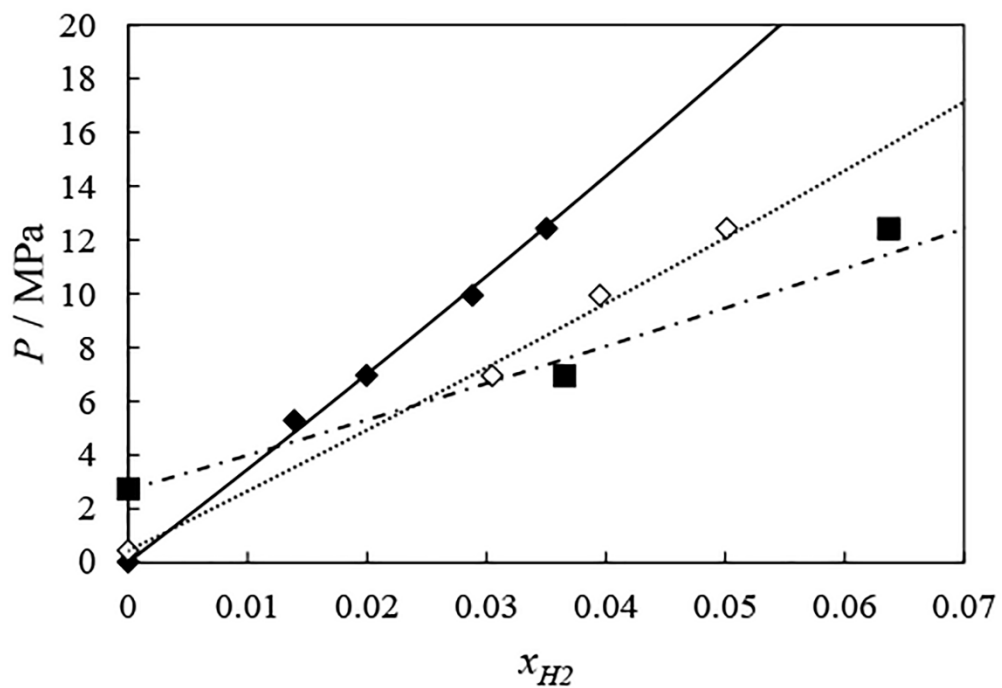| T / K	Binary interaction parameter k_{ij} for H_2+furfural	Binary interaction parameter k_{ij} for H_2+2-propanol
323.5	-0.187	-0.301
399.0	-0.305	-0.255
476.0	-0.199	0.038

Standard uncertainty: $u(T) = 0.2$ K.

Figure 2. Hydrogen solubility in 2-propanol: at 323.4 K (♦), 399.1 K (◊), and 476.0 K (■). The vapor pressures presented at $x_{H2} = 0$ are obtained from DIPPR correlation.[31] Prediction with PC-SAFT, at 323.4 K (—), at 399.1 K (…), and at 476.0 K (–··–).
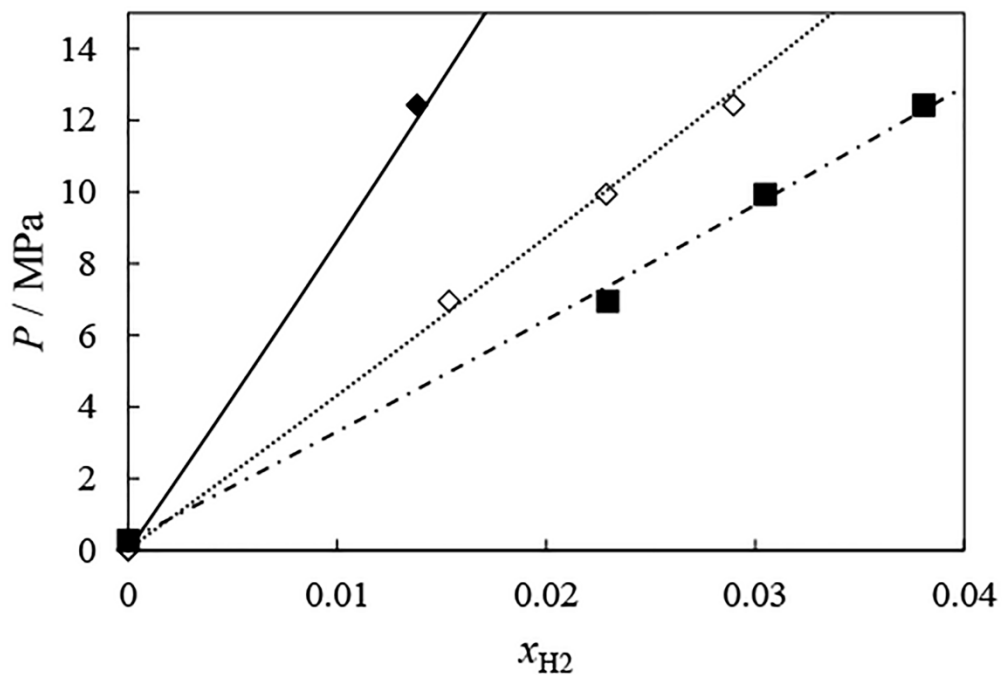
Figure 3. Hydrogen solubility in furfural: at 323.1 K ($\blacklozenge$), 399.2 K ($\lozenge$), and 476.1 K ($\blacksquare$). The vapor pressures presented at $x_{H2} = 0$ are obtained from DIPPR correlation.[31] Prediction with PC-SAFT, at 323.1 K (—), at 399.2 K (…), and at 476.1 K (– · –).

PC-SAFT with temperature dependent interaction parameter for H_2 + 2-propanol predicted hydrogen solubility in 2-propanol well in lower temperatures with an absolute average deviation of 0.21 MPa at 323.4 K and 0.32 MPa at 399.1 K. However, at 476.0 K the prediction accuracy decreased to AAD of 0.79 MPa. PC-SAFT with temperature dependent binary interaction parameter for H_2 + furfural predicted hydrogen solubility well at temperatures of 323.1, 399.2, and 476.1 K. The absolute average deviation at these temperatures were 0.24, 0.33, and 0.31 MPa, respectively. Furthermore, calculated vapor pressures of furfural and 2-propanol in various temperatures were observed to be well predicted with PC-SAFT.

Hydrogen solubility in 2-propanol was measured by Lühring et al. [12] at 293.2 K and Krüger et al. [13] at 298.15 K at atmospheric pressure. Due to the higher measurement temperatures and pressures in this work, the hydrogen solubility data in the references is not directly comparable. In the study by Lühring et al. [12] hydrogen solubilities are presented as Henry`s constants. This constant was applied to calculate hydrogen solubilities in higher pressures. For data presented in the study by Krüger et al. [13] an assumption was made that the solubilities follow Henry`s law. The results obtained in this study were plotted together with the literature data at two isobaric conditions (12.47 and 6.97 MPa) as a function of temperature. The comparisons are presented in Figure 4. A clear trend is visible for hydrogen solubility in 2-propanol as a function of temperature, and the hydrogen solubility measurement data presented in this study is well in line with the literature data.
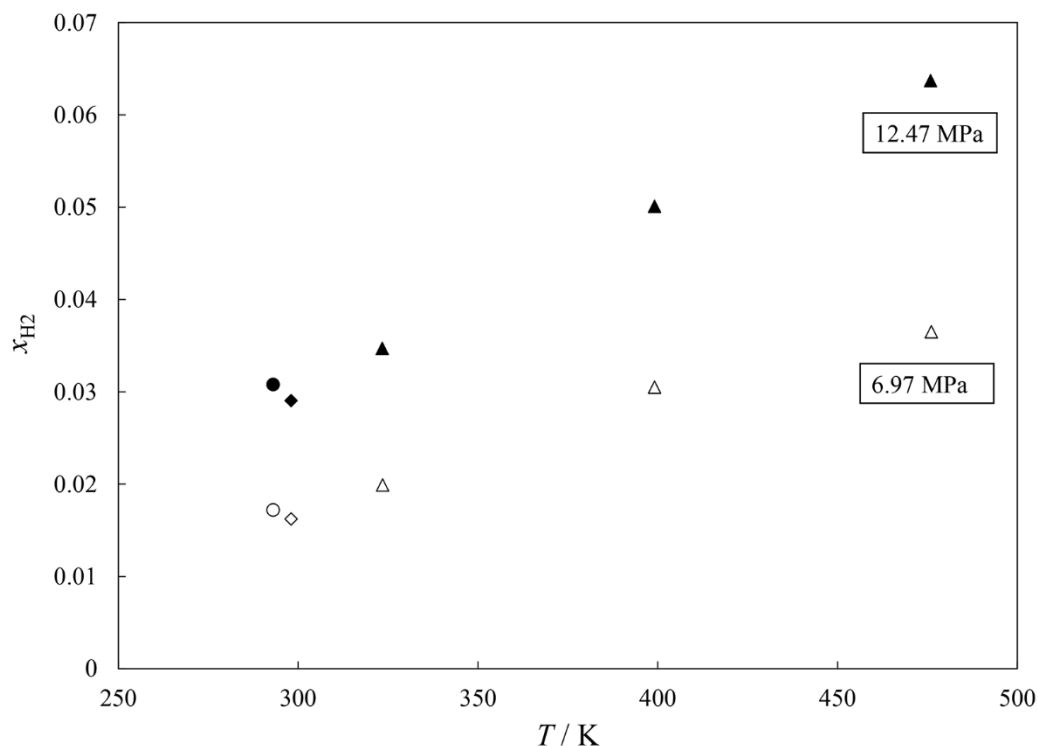
Figure 4. Comparison of hydrogen solubility in 2-propanol at isobaric conditions. Comparison at 12.47 MPa: ref [12] (●), ref [13] (♦), this work (▲). Comparison at 6.97 MPa: ref [12] (○), ref [13] (◊), this work (Δ).

The purity of relatively unstable furfural was analyzed after hydrogen solubility experiments. GC-results indicated that only small amount of reactions of furfural occurred at 323 or 399 K. However, at reaction temperature of 476 K more hydrogenation reactions were observed. GC-MS analysis indicated that the products formed in the higher temperature were mainly furfuryl alcohol and 2-methylfuran. Approximately 4.6 % of furfural was analyzed to have converted into products during the measurement at 476 K. The GC chromatograms of pure furfural and furfural after 399 K and 476 K experiments are presented in the supporting information (Figures S1-S3). The 2-propanol impurity presented in the Figures S2 and S3 originates from the stabilization pump, as this component was applied to wash the equipment before the experiments. The 2-butanol was used as an internal standard and is thus present in the GC-graphs. The reactivity of furfural at 476 K might have influenced the results slightly, which might also be an explanation for the smaller binary interaction parameter k_{ij} for furfural + H_2 mixture in Table 7. However, the reactivity of furfural was considered negligible concerning the measurements at 323 and 399 K and its effect on the modeling.

4. Conclusions

This study investigated the formerly unstudied hydrogen solubility in furfural as well as hydrogen solubility in a commonly applied solvent, 2-propanol. The measurements performed for this study were conducted at the temperature range of 323 – 476 K and pressure range of 0.3 – 12.5 MPa. The measurements were compared to predictions by SRK, PR, and PC-SAFT models. From these, PC-SAFT model predicted hydrogen solubility data most accurately after binary interaction parameter regression. Without binary interaction parameter regression the PC-SAFT and other equation of state models lacked predictive capability. Thus, it can be concluded the experimental data together with binary interaction parameter regression is very important to obtain predictive behavior with PC-SAFT or any other EoS for these components. Insignificant thermal reactions of furfural occurred at temperatures below 399 K, but at 476 K furfural hydrogenation products (furfuryl alcohol, 2-methylfuran) were detected. The amount of reacted furfural remained under 5 % during the experiments even at the highest temperature. The data presented in this paper provides important information for modeling hydrotreatment reactions of furfural for the production of chemicals and biofuels.

5. Acknowledgements

6. References

[1] R. Karinen, K. Vilonen, M. Niemelä, Biorefining: Heterogeneously catalyzed reactions of carbohydrates for the production of furfural and hydroxymethylfurfural, ChemSusChem 4 (2011) 1002-1016.

[2] D. Kubicka, I. Kubickova (Eds.), Furfurals as chemical platform for biofuels production, in: D.E. Resasco, S. Sitthisa, J. Faria, T.Prasomsri, M. Pilar Ruiz Heterogeneous Catalysis in Biomass to Chemicals and Fuels, Research Signpost, India, 2011, pp. 1-33.

[3] C. M. Cai, T. Zhang, R. Kumar, C.E. Wyman, Integrated furfural production as a renewable fuel and chemical platform from lignocellulosic biomass, J. Chem. Technol. Biot. 89 (2013) 2-10.

[4] J.P. Lange, E. van der Heide, J. van Buijtenen, R. Price, Furfural - A promising platform for lignocellulosic biofuels, ChemSusChem 5 (2012) 150-166.

[5] H.Y. Zheng, Y.L. Zhu, B.T. Teng, Z.Q. Bai, C.H. Zhang, H.W. Xiang, Y.W. Li, Towards understanding the reaction pathway in vapour phase hydrogenation of furfural to 2-methylfuran, J. Mol. Catal. A. Chem. 246 (2006) 18 - 23.

[6] P. Panagiotopoulou, D.G. Vlachos, Liquid phase catalytic transfer hydrogenation of furfural over a Ru/C catalyst, Appl. Catal. A. 480 (2014) 17-24.

[7] V. Choudhary, A.B. Pinar, S.I. Sandler, D.G. Vlachos, R.F. Lobo, Xylose isomerization to xylulose and its dehydration to furfural in aqueous media, ACS Catal. 1 (2011) 1724-1728.

[8] X. Chang, A.-F. Liu, B. Cai, J.-Y. Luo, H. Pan, Y.-B. Huang, Catalytic Transfer Hydrogenation of Furfural to 2-Methylfuran and 2-Methyltetrahydrofuran over Bimetallic Copper-Palladium Catalysts, ChemSusChem 9 (2016) 1 – 9.

[9] J. Kijenski, P. Winiarek, T. Paryjczak, A. Lewicki, A. Mikolajska, Platinum deposited on monolayer supports in selective hydrogenation of furfural to furfuryl alcohol, Appl. Catal. A. 233 (2002) 171 – 182.

[10] K. Yan, G. Wu, T. Lafleur, C. Jarvis, Production, properties and catalytic hydrogenation of furfural to fuel additives and value-added chemicals, Renew. Sustainable Energy Rev. 38 (2014) 663-676.

[11] Y. Nakagawa, M. Tamura, K. Tomishige, Catalytic reduction of biomass-derived furanic compounds with hydrogen, ACS Catal. 3 (2013) 2655-2668.

[12] J. Lühring, A. Schumpe. Gas solubilities (H_2, He, N_2, CO, O_2, Ar, CO_2) in organic liquids at 293.2 K, J. Chem. Eng. Data 34 (1989) 250-252.

[13] M.B. Krüger, C. Selle, D. Heller, W. Baumann, Determination of gas concentrations in liquids by nuclear magnetic resonance: Hydrogen in organic solvents, J. Chem. Eng. Data 57 (2012) 1737-1744.

[14] G. Soave. Equilibrium constants from a modified Redlich-Kwong equation of state, Chem. Eng. Sci. 27 (1972) 1197-1203.

[15] D.-Y. Peng, D.B. Robinson, A new two-constant equation of state, Ind. Eng. Chem. Fundam. 15 (1976) 59-64.

[16] M. Safamirzaei, H. Modarress, M. Mohsen-Nia, Modeling the hydrogen solubility in methanol, ethanol, 1-propanol and 1-butanol, Fluid Phase Equilib. 289 (2010) 32-39.

[17] J.V.H. d`Angelo, A.Z. Francesconi, Gas-liquid solubility of hydrogen in n-alcohols (1<n 4) at Pressures from 3.6 MPa to 10 MPa and Temperatures from 298.15 K to 525.15 K, J. Chem. Eng. Data 46 (2001) 671-674.

[18] M.H. Kapateh, A.Chapoy, R. Burgass, B. Tohidi, Experimental measurement and modeling of the solubility of methane in methanol and ethanol, J. Chem. Eng. Data 61 (2016) 666-673.

[19] J. Gross, G. Sadowski, Perturbed-chain SAFT: An equation of state based on a perturbation theory for chain molecules, Ind. Eng. Chem. Res. 40 (2001) 1244-1260.

[20] J.A. Barker, D.Henderson, Pertubation theory and equation of state for fluids: A successful theory of liquids, J. Chem. Phys. 47 (1967) 4714.

[21] J.A. Barker, D.Henderson, Pertubation theory and equation of state for fluids: The square-well potential, J. Chem. Phys. 47 (1967) 2856.

[22] W.G. Chapman, K.E. Gubbins, G. Jackson, M. Radosz, New reference equation of state for associating liquids, Ind. Eng. Chem. Res., 29 (1990) 1709.

[23] C.B. Soo, Experimental thermodynamic measurements of biofuel-related associating compounds and modeling using the PC-SAFT equation of state, Thesis, Ecole Nationale Superieure des Mines de Paris, 2011.

[24] T.B. Nguyen, Representation of oxygenated fluids associated with biomass valorization: Descriptor definition, PhD Thesis, L`Université Pierre et Marie Curie, 2013.

[25] X. Liang, I. Tsivintzelis, G.M. Kontogeorgis, Modeling water containing systems with the simplified PC-SAFT and CPA equations of state, Ind, Eng, Chem. Res. 53 (2014) 14493-14507.

[26] W. Feng, H.J. van der Kooi, J. de Swaan Arons, Application of the SAFT equation of state to biomass fast pyrolysis liquid, Chem. Eng. Sci., 60 (2005) 617-624.

[27] D. Nguyen-Huynh, J.-C. de Hemptinne, R. Lugo, J.-P. Passarello, P. Tobaly, Simultaneous liquid-liquid and vapor-liquid equilibria predictions of selected oxygenated aromatic molecules in mixtures with alkanes, alcohols, water, using the polar GC-PC-SAFT, Chem. Eng. Res. Des. 92 (2014) 2912-2935.

[28] M.S. Qureshi, J. Touronen, P. Uusi-Kyyny, D. Richon, V. Alopaeus, Solubility of hydrogen in bio-oil compounds, J. Chem. Thermodyn. 102 (2016) 406-412.

[29] M. Saajanlehto, P. Uusi-Kyyny, V. Alopaeus, A modified continuous flow apparatus for gas solubility measurements at high pressure and temperature with camera system, Fluid Phase Equilib. 382 (2014) 150-157.

[30] M. Saajanlehto. Phase equilibria of heavy oil systems in hydroprocesses: Experiments and modeling, PhD Thesis, Aalto University (FIN) 2015.

[31] R.L. Rowley, W.V. Wilding, J.L. Oscarson, Y. Yang, N.A. Zundel. DIPPR data compilation of pure chemical properties, Design Institute for Physical Properties, Bringham Young University, Provo Utah, 2006.

[32] E. Brunner, Solubility of hydrogen in 10 organic solvents at 298.15, 323.15, and 373.15 K, J. Chem. Eng. Data 30 (1985) 269-273.

[33] J.V.H. d`Angelo A.Z. Francesconi, Salt effect in the solubility of hydrogen in n-alcohols at pressures up to 10 MPa and temperatures up to 498.15 K, Braz. J. Chem. Eng. 17 (2000) 4-7.

[34] P.K. Frolich, E.J. Tauch, J.J. Hogan, A.A. Peer, Solubilities if gases in liquids at high pressure, Ind.Eng. Chem. 23 (1931) 548-550.

[35] T. Katayama T. Nitta, Solubilities of hydrogen and nitrogen in alcohols and n-hexane, J. Chem. Eng. Data 21 (1976) 194-196.

[36] Aspen Technology Inc., Aspen Plus v.8.8 software, 1981.